Published article:

Ross, AN (2011) *Scalar Transport over Forested Hills.* Boundary-Layer Meteorology, 141 (2). 179 - 199. ISSN 0006-8314

http://dx.doi.org/10.1007/s10546-011-9628-y

Boundary-Layer Meteorology manuscript No.
(will be inserted by the editor)

Scalar transport over forested hills

Andrew N. Ross

Received:

Abstract Numerical simulations of scalar transport in neutral flow over forested ridges are performed using both a one-and-a-half order mixing length closure scheme and a large-eddy simulation (LES). Such scalar transport (particularly of CO_2) has been a significant motivation for dynamical studies of forest canopy - atmosphere interactions. Results from the one-and-a-half order mixing length simulations show that hills where there is significant mean flow into and out of the canopy are more efficient at transporting scalars from the canopy to the boundary layer above. For the case with a source in the canopy this leads to lower mean concentrations of tracer within the canopy, although they can be very large horizontal variations over the hill. These

A.N. Ross

Institute for Climate and Atmospheric Science, School of Earth and Environment, University of Leeds, UK.

Tel.: +44-113-3437590

Fax.: +44-113-3435259

E-mail: A.N.Ross@leeds.ac.uk

variations are closed linked to flow separation and recirculation in the canopy and can lead to maximum concentrations near the separation point which exceed those over flat ground. Simple scaling arguments building on the analytical model of Finnigan and Belcher (2004, Q. J. Royal Meteorol. Soc. 130:1-29) successfully predict the variations in scalar concentration near canopy top over a range of hills. Interestingly this analysis suggests that variations in the components of the turbulent transport term, rather than advection, give rise to the leading order variations in scalar concentration. The scaling arguments provide a quantitative measure of the role of advection, and suggest that for smaller / steep hills and deeper / sparser canopies advection will be more important. This agrees well with results from the numerical simulations.

A LES is used to support the results from the mixing-length closure model and to allow more detailed investigation of the turbulent transport of scalars within and above the canopy. Scalar concentration profiles are very similar in both models, despite the fact that there are significant differences in the turbulent transport, highlighted by the strong variations in the turbulent Schmidt number both in the vertical and across the hill in the LES which are not represented in the mixing length model.

Keywords Flow over a hill; Forest canopy; Large-eddy simulation; Scalar transport

1 Introduction

In recent years there has been significant interest in the dynamics of forest canopy–boundary layer interactions over complex terrain. A significant motivation for this work has been to understanding advective effects in flux measurements (notably CO_2) over forest canopies and to improve the flux estimates as a result (see Finnigan, 2008, and other papers in the same invited feature). The analytical work of Finnigan and Belcher (2004) has been an important step in understanding these dynamics. Finnigan and Belcher (2004) extended the linear theory of Hunt et al. (1988) for neutral flow over a hill to include the effects of a forest canopy. They demonstrated the ubiquity of flow separation in deep canopies. The analytical solutions break down for small hills when advection at canopy top became comparable to the perturbation shear stress divergence at leading order. Subsequent numerical simulations by Ross and Vosper (2005) using a one-and-a-half order turbulence closure scheme demonstrated that in these cases vertical advection at canopy top is important at leading order. Streamlines show flow into the canopy over the upwind slope and out of the canopy just downwind of the hill crest. This led to a feedback between the canopy flow and the larger scale pressure field over the hill, with a subsequent downwind shift in the surface pressure field, an increase in pressure drag and a downwind shift in the maximum near-surface speedup over the hill. Similar conclusions were drawn from large-eddy simulations (LES) of flow over a small hill (Ross, 2008) using the same model and LES by Patton and Katul (2009). Other large-eddy simulations (Dupont et al., 2008) have reproduced the wind tunnel experiments of Finnigan and Brunet (1995). These large-eddy simulations do not rely on the use of a first order canopy turbulence closure scheme, which has been a topic of some debate in the literature (Finnigan, 2000; Pinard and Wilson, 2001; Katul et al., 2004).

Experimental observations are still relatively rare, with the only significant wind tunnel study both within and above a canopy over a hill being that of Finnigan and Brunet (1995). Recent water flume experiments (Poggi and Katul, 2007c,b,a) have provided more detailed measurements and support many of the conclusions drawn from the modelling work. They have also provided important measurements of the unsteady nature of the canopy flow, particularly in the recirculation region (Poggi and Katul, 2007a).

The impact of this dynamical work for those measuring fluxes is summarised in the paper of Belcher et al. (2008). From an analytical point of view, applying this theoretical work to study scalar transport has been difficult as scalar profile observations above forest do not agree with simple boundary-layer theory even over flat terrain, although some recent progress has been made here (Harman and Finnigan, 2008). Katul et al. (2006) have attempted to consider the impact of the dynamics on CO_2 fluxes using an ecophysical canopy model driven by a simplified analytical wind field based on Finnigan and Belcher (2004). This demonstrates the impact that the dynamics can have on scalar concentrations and fluxes, however unfortunately the small hill and canopy they used to demonstrate the results (the same one used in Finnigan and Belcher, 2004; Ross and Vosper, 2005) violates the assumptions of the full analytical model, let alone the simplified version they adopt. Observational studies, notably the ADVEX (ADVection EXperiment) project (Feigenwinter et al., 2008), have begun to investigate the impact of advection for flux sites. Some of these studies, for example Zeri et al. (2010), provide qualitative support for the theoretical predictions of Finnigan and Belcher (2004) and Katul et al. (2006). With all this in mind, there is still need for a systematic assessment of the impact of the canopy dynamics on scalar transport over hills, which this paper seeks to address.

While there is debate in the literature about whether first order turbulence closure schemes should be used for canopy flows, from a practical point of view they are useful. They are simple enough that they are amenable to analytical analysis (e.g. Finnigan and Belcher, 2004) and computational cheap enough to allow realistic simulations to be conducted. Studies such as Pinard and Wilson (2001); Katul et al. (2004); Ross (2008) have shown that in terms of the mean flow they produce similar results to higher order closure schemes, to large-eddy simulations and to experiments. This is principally because they correctly reproduce the canopy-top turbulence which dominates the canopy flow. They do less well in terms of representing the turbulence deep in the canopy (e.g. Ross, 2008), but this is not significant for the mean flow since the mean velocity gradients are low in that region. In terms of scalar transport the picture is less clear. There may be significant gradients in the scalar concentration deep in the canopy depending on the sources and sinks, and hence there may be more significant errors in the turbulent scalar fluxes. There are also questions about the behaviour of the turbulent Schmidt number (the ratio of the turbulent diffusivities for momentum and scalars) within and just above the canopy (see e.g. Harman and Finnigan, 2008). Nonetheless the fact that first order closure schemes are amenable to analytical study allows a more complete analysis of the role of advection in scalar transport. While the results of such models may not exactly represent reality they offer a useful guide to likely different flow regimes and scalings which can be tested against observations or limited numerical results from models with more complex turbulence schemes. Finally, since such simple models are being used practically through computational necessity, it is valuable to understand their behaviour and possible limitations and to seek ways of improving them. For these reasons this paper will primarily concentrate on first order closure models of scalar transport, although comparison will be made with a large-eddy simulation in section 5.

Section 2 will describe the numerical model used here and the simulations of passive scalar transport. Section 3 will present some simple scaling arguments based on the analytical model of Finnigan and Belcher (2004) for flow over a canopy-covered hill. This provides some insight into the dominant processes controlling variations in scalar concentration and flux in the upper canopy and in the boundary layer above. Results of the first order simulations are presented and discussed in section 4 and compared with the scaling arguments developed. Limitations of first order closure schemes are discussed, and to partly address this results from a large eddy simulation are presented in section 5 for comparison. Section 6 discusses the implications of this work for flux measurements and finally section 7 offers some conclusions and topics for further study.

2 Simulations of passive scalar transport

2.1 Model description

Simulations were carried out using the BLASIUS model from the UK Met Office (Wood and Mason, 1993). The model can be run with a first-order or a one-and-a-half order mixing length turbulence closure scheme. It can also be used for large-eddy simulations. It has previously been used in both modes for studying the dynamics of flow over canopy-covered hills (Ross and Vosper, 2005; Ross, 2008; Brown et al., 2001).

For all the simulations presented here an idealised two-dimensional, sinusoidal, periodic hill is used with the hill surface, z_s, given by

$$z_s = \frac{H}{2}\cos(kx) \tag{1}$$

where H is the height of the hill, $k = \pi/(2L)$ is the hill wavenumber and L is the half width of the hill at half height. The length of the domain is always $4L$, i.e. the domain contains exactly one hill. Neutral flow is assumed in all cases and periodic boundary conditions are used meaning that the simulations actually represent neutral flow over an infinite series of sinusoidal ridges. In all the simulations presented here the domain has 128 grid points in the horizontal. For the majority of simulations the domain depth is fixed at 1500 m. A stretched grid with 80 grid points is used in the vertical with a resolution of 0.5 m near the surface increasing gradually to 33.5 m at domain top.

A uniform canopy density, $a = 0.2 - 0.6\,\mathrm{m}^{-1}$ and a fixed canopy drag coefficient ($C_d = 0.25$ or $C_d = 0.15$) were used for all simulations. This gives values for the canopy adjustment length, $L_c = 1/(C_d a)$ of $6.67\,\mathrm{m} - 26.7\,\mathrm{m}$. Unless otherwise stated the canopy height $h = 10\,\mathrm{m}$, although some simulations are conducted with $h = 5\,\mathrm{m}$ or $h = 20\,\mathrm{m}$. These canopy parameters are all representative of observations in real forests and correspond to values used in previous theoretical work, allowing direct comparison. The flow is driven by a horizontal pressure gradient corresponding to a geostrophic wind speed of $10\,\mathrm{m\,s}^{-1}$. Full details of the parameter values used in the simulations are given in §4. The simulations are consistent with those presented in Ross and Vosper (2005) and Ross (2008) allowing direct comparison of the results.

The mixing length closure simulations presented in the first part of this paper were all conducted with the one-and-half order closure scheme with a prognostic equation for turbulent kinetic energy. Full details of the scheme are given in Ross and Vosper (2005). The one-and-a-half order closure scheme requires an additional empirical parameter, β, which measures the ratio of friction velocity to mean wind at canopy top, to be specified. For most simulations this is taken as 0.3, as in Ross and Vosper (2005) and consistent with observations over real forests. This parameter controls the relationship between L_c, the canopy mixing length, l, and displacement height, d, as described in Finnigan and Belcher (2004) and Ross and Vosper (2005). The effect of modifying β is studied in section 5 and compared to results using a LES.

In section 5 the model is used to conduct large-eddy simulations. The model setup is identical to that described in Ross (2008), and the reader is referred to that paper for a full discussion of the requirements for a successful LES and the model setup. The requirements to adequately resolve the larger eddies in the canopy places a strong limitation on the number of cases, the canopy and the size of hills that can be modelled. For these reasons the hill is taken as $H = 10\,\mathrm{m}$ and $L = 100\,\mathrm{m}$. The canopy has $C_d = 0.15$, $a = 0.25\,\mathrm{m}^{-1}$ and $h = 20\,\mathrm{m}$. The domain height is limited to 132 m. The domain has $288 \times 192 \times 96$ grid points, giving a horizontal and vertical grid spacing of 1.39 m. This differs from the majority of the mixing length simulations described in this paper, and is a result of the computational limitations imposed by the LES. Where direct comparison is made between the LES and mixing length closure results, the mixing length closure simulations have been performed with an identical model setup in terms of domain size, hill size and canopy parameters, although the horizontal resolution is slightly lower.

2.2 Scalar releases

The majority of the simulations presented in the paper involve a constant uniform release rate for a passive scalar tracer within the canopy. In order to allow a steady-state solution a sink of equal magnitude is distributed over the top 500 m of the domain to balance the source. For the simulations using the shallow LES domain, the sink is over the top 20 m of the domain. Zero flux boundary conditions are used at the ground and at the top of the domain so the total tracer in the domain is conserved. In this case the units of the tracer are arbitrary, however a canopy release rate of $10^{-2}\,\mathrm{m}^{-3}\,\mathrm{s}^{-1}$ is used. A one-dimensional simulation is run with the tracer concentration initially set to 1 throughout the domain. Once this simulation has reached a near-equilibrium state then the profiles are used to initialise the two-dimensional simulations. The same tracer setup is used for the large-eddy simulations described in §5 .

3 Scaling arguments for the importance of advection

There are four independent length scales in the problem (H, L, h and L_c). The canopy mixing length, l, is proportional to the canopy adjustment length, L_c, so is not independent. These length scales give three non-dimensional parameters controlling the dynamics of flow over a forested hill, namely the hill slope, H/L, the ratio of the hill width to the canopy adjustment length scale, L/L_c, and β times the canopy depth non-dimensionalised on the canopy mixing length, $\beta h/l$. Note the inclusion of the non-dimensional empirical parameter, β, is for convenience since it is this group which appears in the analytical solution for the background flow and for the perturbations over the hill in Finnigan and Belcher (2004).

The turbulent transport equation for a scalar tracer, c, in a turbulent canopy flow can be written as

$$\frac{Dc}{Dt} = \frac{\partial}{\partial x_i}\left(K_c \frac{\partial c}{\partial x_i}\right) + S \tag{2}$$

using a first order turbulence closure with K_c the eddy viscosity or turbulent diffusivity for scalars. S is the source / sink term for the scalar tracer. Here molecular diffusion is neglected. In a homogeneous, steady flow then the source / sink term is exactly balanced by the divergence of the vertical scalar flux term and so

$$S = -\frac{\partial}{\partial z}\left(K_c \frac{\partial c}{\partial z}\right). \tag{3}$$

Following other recent theoretical and modelling studies (e.g. Finnigan and Belcher, 2004; Ross and Vosper, 2005), consider two-dimensional flow over a series of sinusoidal ridges covered by a uniform canopy. The flow can be considered as a mean horizontal flow $U(z)$ plus a perturbation $(u(x,z), w(x,z))$. Finnigan and Belcher (2004) give an analytical solution for this perturbed flow within and above the canopy. Similarly the scalar concentration may be considered as a mean value, $C(z)$ plus a perturbation, $c(x,z)$. All perturbations are assumed small, allowing the transport equation to be linearised.

For the homogeneous, flat ground case then from Finnigan and Belcher (2004) we get

$$U(z) = \begin{cases} U_h e^{\beta z/l} & z < 0 \\ \frac{u_*}{\kappa} \log\left(\frac{z+d}{z_0}\right) & z >= 0 \end{cases} \tag{4}$$

and

$$K_c = l_m^2 \frac{dU}{dz} = \begin{cases} \beta l U_h e^{\beta z/l} & z < 0 \\ u_* \kappa (z+d) & z >= 0. \end{cases} \tag{5}$$

where l_m is the mixing length, which is constant within the canopy and scales with height above, u_* is the friction velocity and U_h is the velocity at canopy top. The displacement height d and the roughness length z_0 are determined from β and l. Substituting this into the equation (3) and integrating gives

$$\frac{dC}{dz} = \begin{cases} -\frac{Sh}{\beta l U_h}\left(1+\frac{z}{h}\right) e^{-\beta z/l} & z < 0 \\ -\frac{c_*}{\kappa(z+d)} & z >= 0 \end{cases} \tag{6}$$

and

$$C = \begin{cases} \frac{Sh}{\beta^2 U_h}\left(1+\frac{z}{h}+\frac{l}{\beta h}\right) e^{-\beta z/l} - \frac{Sh}{\beta^2 U_h}\left(2+\frac{l}{\beta h}\right) + c_1 & z < 0 \\ -\frac{c_*}{\kappa}\log\left(\frac{z+d}{z_0}\right) + c_1 & z >= 0 \end{cases} \tag{7}$$

for some constant c_1, where $Sh \equiv u_* c_*$, assuming that $\partial C/\partial z = 0$ at $z = -h$.

From Finnigan and Belcher (2004) we may take the analytical solution for the perturbed velocity and eddy viscosity. This solution is valid when $H/L \ll 1$, $\beta h/l \gg 1$ and $kL_c \exp(\beta h/l) \ll 1$. Assuming perturbations in the scalar are also small, we may linearise about the perturbations in both the scalar and velocity fields to give

$$U\frac{\partial c}{\partial x} + w\frac{\partial C}{\partial z} = \frac{\partial}{\partial x}\left(K_c \frac{\partial c}{\partial x}\right) + \frac{\partial}{\partial z}\left(K_c \frac{\partial c}{\partial z} + K_c' \frac{\partial C}{\partial z}\right). \tag{8}$$

The linearised eddy viscosity terms can be written in terms of the velocity field (see Finnigan and Belcher, 2004) as

$$K_c = l_m^2 \frac{dU}{dz} \quad \text{and} \quad K_c' = l_m^2 \frac{\partial u}{\partial z}. \tag{9}$$

In the upper canopy and just above the canopy horizontal derivatives scale on the horizontal length scale L while vertical derivatives scale on the mixing length, l. Using this we see that the first term on the right hand side of (8) is small ($O(l^2/L^2)$) compared to the second term. Similarly, the first and second terms on the left hand side are small ($O(l/L)$) compared to the second and third terms respectively on the right hand side, and so may be neglected. This also makes use of the continuity equation to scale $w \sim ul/L$. This leaves a balance between the two components of the vertical turbulent transport perturbation term on the right hand side. Equating these two terms and integrating gives

$$\frac{\partial c}{\partial z} = \frac{c_*}{u_*}\frac{\partial u}{\partial z} \tag{10}$$

and so

$$c = \frac{c_*}{u_*}u + c_0(x) \tag{11}$$

for some function $c_0(x)$. Taking the expression for u from Finnigan and Belcher (2004) and assuming that the contribution, $c_0(x)$ from the deep canopy is small, or at least scales in the same way, gives

$$c \sim \frac{Sh}{U_h}\frac{H}{L}\frac{L_c}{L}\frac{U_0^2}{U_h^2} \tag{12}$$

near canopy top. Here U_0 is the velocity at the middle layer height and gives a velocity scale for the outer flow. See Finnigan and Belcher (2004) for details. Note that this scaling means that the leading order ($O(l/L)$) correction to the tracer field resulting from the hill results from a balance between the changes in the turbulent transport term due to changes in the tracer profile and changes in the eddy viscosity. At leading order there is no net change in the turbulent flux. Changes in the turbulent flux must come from a second order balance ($O(l^2/L^2)$) with the advection term.

Using this scaling the magnitude of the tracer advection term can be derived as

$$U\frac{\partial c}{\partial x} \sim S 2\beta^2 \frac{\beta h}{l}\frac{H}{L}\frac{L_c^2}{L^2}\frac{U_0^2}{U_h^2} \tag{13}$$

near canopy top. This allows direct estimation of the importance of advection compared to the canopy source term, S.

4 Tracer concentrations and fluxes over complex terrain

A large number of simulations with a constant tracer release were carried out over a range of different parameter values. These are summarised in table 1. In particular simulations corresponding to the narrow and wide hill examples discussed in Ross and Vosper (2005) were performed. The tracer profiles for these simulations are shown below.

Figure 1 shows horizontally-averaged vertical profiles of relative tracer concentration compared to the flat ground case for various experiments given in table 1. In all simulations the horizontally-averaged scalar flux is the same and constant with height since the sources and sinks of the scalar are fixed and the simulations are run to a quasi-steady state, however there are clear differences in the horizontally-averaged scalar concentrations. Figure 1(a) shows results for 4 simulations with different slopes H/L and fixed hill width and canopy parameters ($L/L_c = 10$ and $\beta h/l = 5.55$). This

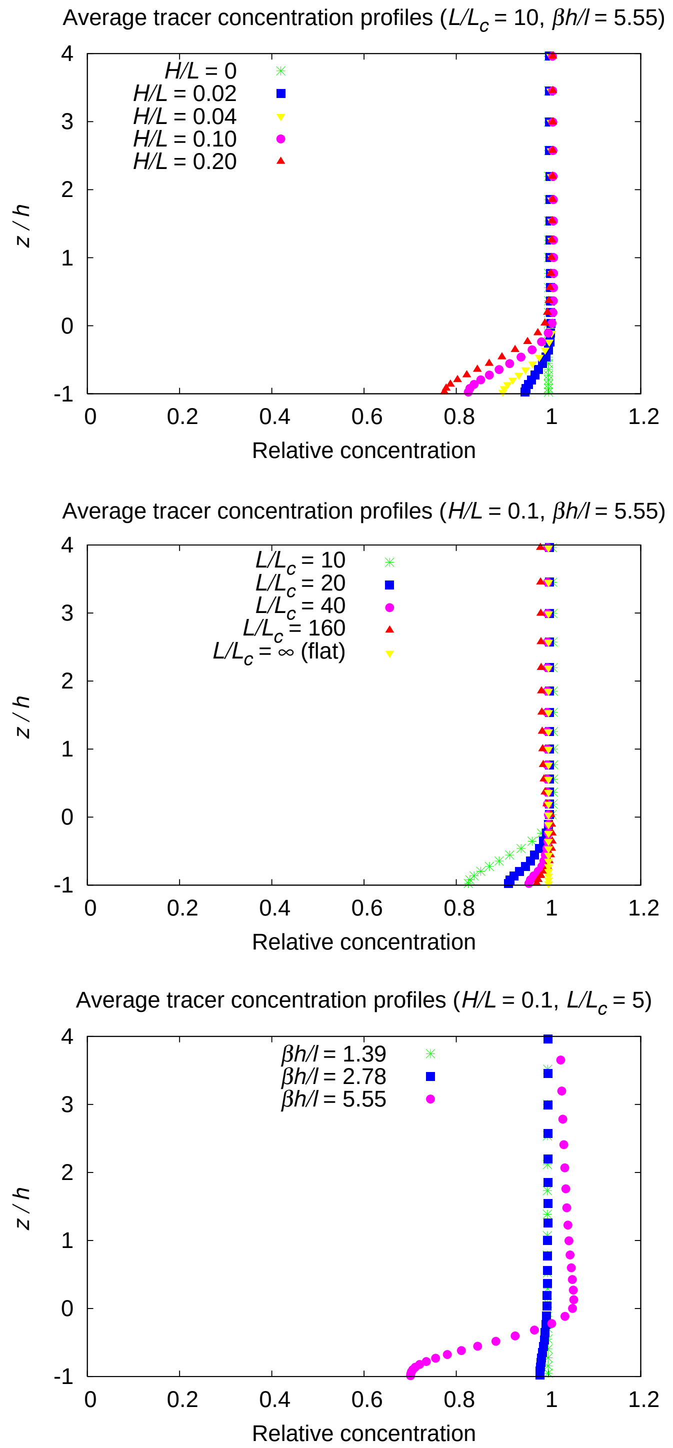

Fig. 1 Horizontally-averaged vertical profiles of tracer concentration relative to the equivalent profile over flat ground. Height is non-dimensionalised on the canopy height, h. Canopy top is at $z/h = 0$. The top figure shows profiles for a fixed canopy and hill width, but for different hill heights, i.e. increasing slope, H/l. The middle figure shows profiles for a fixed slope and canopy, but for different scale hills. The bottom figure shows profiles for a fixed hill and different canopy depths.

Table 1 Hill and canopy parameters for the various two-dimensional mixing length closure simulations performed.

Parameter	Values
L	$100-1600\,\mathrm{m}$
a	$0.2-0.6\,\mathrm{m}^{-1}$
h	$5-20\,\mathrm{m}$
H/L	0.00625 - 0.2
L/Lc	3.75 - 240
$\beta h/l$	1.39 - 8.33

corresponds to the small hill width case described in Ross and Vosper (2005) where vertical advection at canopy top is important. Increasing the slope leads to greater vertical velocities into and out of the canopy and so increases the tracer transport by the mean flow. This gives significantly lower average concentrations of tracer within the canopy compared to the flat ground case, and slightly higher concentrations above. Figure 1(b) shows profiles for 5 simulations with fixed $H/L = 0.1$ and $\beta h/l = 5.55$ and varying L/L_c, i.e. fixed slope and canopy parameters and varying hill width. Here decreasing L/L_c (i.e. smaller hill widths compared to the canopy adjustment scale L_c) again leads to an increase in vertical advection at canopy top, increased tracer transport and lower averaged concentrations within the canopy. Finally figure 1(c) shows profiles for 3 simulations with fixed $H/L = 0.1$, $L/L_c = 5$ and varying $\beta h/l$, i.e. fixed slope, hill width and canopy density and varying canopy height. Increasing the canopy height leads to a deeper region of flow convergence / divergence in the canopy and hence, by continuity, a greater vertical velocity at canopy top. This is turn increases tracer transport and leads to a significant reduction in tracer concentration within the canopy and a slight increase above. Note that only the simulation with the deepest canopy demonstrates a strong increase in tracer concentration above the canopy. In all other cases the additional tracer from within the canopy is redistributed over a sufficient depth in the boundary layer that the increases in concentration are not large. For the $\beta h/l = 1.39$ case the canopy is sufficiently shallow that no flow separation occurs. These cases with $L/L_c = 5$ are an extreme example. For wider hills with larger values of L/L_c (not shown) the relative changes in average concentration are smaller, but a broadly similar effect is seen. Deep in the canopy the average tracer concentrations are reduced as a result of the induced flow. This is more pronounced for deeper canopies where the induced flow is larger. In the upper canopy the change in tracer concentration is less for most simulations. For the deepest canopies however an increase in average concentration is observed as in the small L/L_c case.

Overall these simulations demonstrate reductions in mean scalar concentration deep within the canopy (for a canopy source of tracer) resulting from more efficient transport between the canopy and the boundary layer above for steep and / or narrower hills and for deeper / denser canopies. For the cases with the deepest canopy there can actually be an increase in mean scalar concentration near canopy top. These features can be attributed to an increase in the average vertical transport by the mean flow between the canopy and the boundary layer above and is entirely in according with expectations based on the analytical work of Finnigan and Belcher (2004) and numerical simulations of Ross and Vosper (2005). For the case of a tracer sink within the canopy (as is the case for CO_2) then the signs of the changes would be expected to be reversed so higher concentrations would be observed deep within the canopy.

Figures 2(a) and (b) shows colour contour plots of the scalar concentration for 2 simulations - a small ($L/L_c = 10$) and large ($L/L_c = 160$) hill, both with slope $H/L = 0.1$ and $\beta h/l = 5.55$. Also plotted in (c) for comparison are the results over flat ground. The figures are plotted in a terrain following coordinate system so that the vertical axis is height above the surface. This allows direct comparison of the two figures, despite the differences in scale of the two hills. The figures also show the streamlines of the flow. In both cases the streamlines entering and leaving the canopy indicate significant vertical advection at canopy top ($z/h = 0$). Note that the spacing of the streamfunction contours is different within (solid lines) and above (dotted lines) the canopy. This reflects the fact that velocities within the canopy are much smaller than those above. The canopy-averaged results in figure 1 show that the mean concentration in the canopy is reduced in both cases compared to the simulation over flat ground, particularly for the small hill case. Figure 2 shows that this mean value disguises the significant horizontal variations in scalar concentration that occur throughout the canopy.

In both cases concentrations deep in the canopy over the upwind slope are decreased as a result of advection of lower concentration air from above the canopy being transported down into the canopy and the high concentration air within the canopy being transported up out of the canopy both through advection and enhanced turbulent mixing. In general the concentrations in the recirculation region over the lee slope are higher, particularly near the separation and reattachment points. The precise

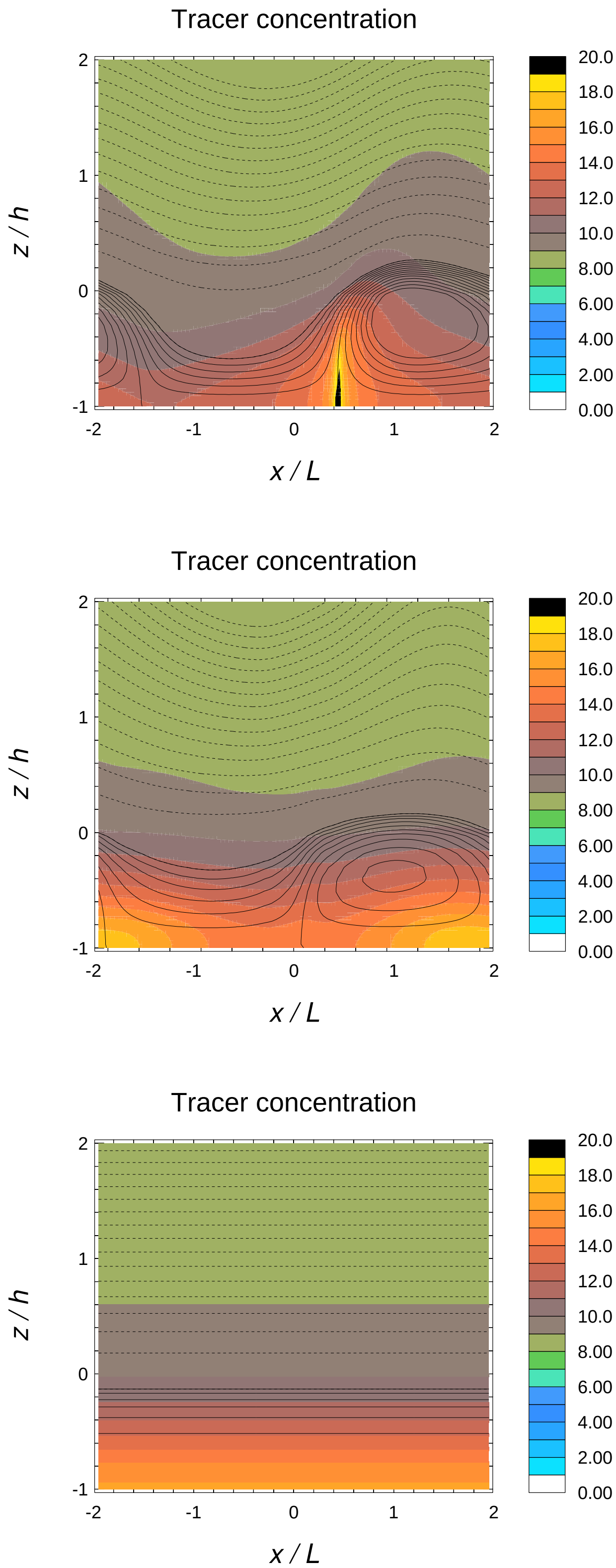

Fig. 2 Scalar concentration (colours) and streamlines (lines) over (a) a small hill ($L = 100\,\mathrm{m}$), (b) a large hill ($L = 1600\,\mathrm{m}$) and (c) flat ground. In both (a) and (b) the hill slope is the same ($H/L = 0.1$) and the canopy is the same ($L_c = 10\,\mathrm{m}^{-1}$ and $\beta h/l = 5.55$). The scalars are plotted in a terrain following coordinate system. Streamlines are plotted as lines of constant streamfunction with the solid contours at intervals of $0.2\,\mathrm{m}^2\mathrm{s}^{-1}$ (mostly within the canopy) and the dotted contours at intervals of $5\,\mathrm{m}^2\mathrm{s}^{-1}$ (mostly above the canopy). This reflects the small velocities within the canopy compared to above.

location and magnitude of the maximum concentration varies between the two simulations. For the small hill (a) there is a tall thin band near the separation point at the front of the recirculation region with very high concentrations. The high concentration is associated with the stagnation of the flow near the separation point. Although the mean concentration in the canopy is lower than the case over flat terrain, the maximum concentration near the stagnation point is higher than values in the canopy over flat terrain. In contrast, over the large hill (b) the maximum concentration is a much wider and shallow region located at the back of the recirculation region near the reattachment point. For intermediate hill widths (not shown) there are maxima in concentration at both locations, with both maxima slightly weaker.

Deep in the canopy velocities and turbulent transport are small in the background state, and the low mean velocity fields mean that there is little advection. Any induced background flow will therefore have a significant impact on tracer concentrations through a combination of advection and changes in turbulent transport. The separation and reattachment points are both stagnation points of the flow and these regions are therefore associated with low flow velocities and with reduced eddy viscosities (and hence lower turbulent transport). This would tend to suggest that concentrations would be highest in these regions, as observed. Whether or not the maximum is at the separation or reattachment point seems to be rather sensitive to the details of the flow and the turbulence scheme. Analysis of a number of simulations shows that the minima in eddy viscosity at these two stagnation points are always quite similar in magnitude, but that the maximum concentration corresponds to the smallest values of this eddy viscosity. In many cases the concentrations actually increase at the other stagnation point.

A more quantitative analysis of this across all the simulations supports this broad picture. Scaling analysis using the solution of Finnigan and Belcher (2004) gives the ratio of vertical advection to the pressure gradient term in the upper canopy as

$$\lambda = \frac{\pi}{4}\frac{L_c}{L}\exp\left(\frac{\beta h}{l}\right) \tag{14}$$

(equation 36 in Finnigan and Belcher, 2004). The relationship between the location of the maximum scalar concentration in the canopy and the role of vertical advection can be quantified through the non-dimensional parameter which is required to be small in order that the vertical velocity at canopy top is negligible in the analytical model (Finnigan and Belcher, 2004; Ross and Vosper, 2005). Figure 2 suggests that the maximum tracer concentrations are closely linked with the separation region in the lee of the hill crest. To explore this figure 3(a) shows the location of the maximum tracer concentration relative to the separation point, $\xi = (x - x_s)(x_r - x_s)$, plotted against λ. Here x_s is the separation point and x_r the reattachment point so a value of 0 for ξ means the maximum occurs at the separation point, while a value of 1 denotes the reattachment point. The figure clearly delineates two regimes. For cases where $\lambda > 5$ the maximum surface concentration occurs very close to the separation point. For simulations where $\lambda \ll 5$ then the maximum concentration occurs near (but usually just upwind of) the reattachment point. In these cases the separation region is sufficiently weak that the maximum in scalar concentration occurs near the bottom of the hill or at the trailing attachment point of the separation region ($x_{trmax} \sim 2$). Looking at individual cases it is clear that λ is not the sole quantity determining the location of flow separation. For a given canopy and hill width λ is fixed (e.g. simulations with $\lambda \sim 20$). Varying the hill height (and hence slope) still has an impact on the location of the flow separation, and hence the maximum in scalar concentration (as shown, for example, in Ross and Vosper, 2005). Increasing the hill slope tends to shift the separation point closer to the hill summit as the stronger adverse pressure gradient promotes earlier flow separation. In each case the scalar maximum is very close to the separation point as shown in figure 3(a). For very sparse canopies increasing the hill height can control whether or not separation occurs. This is seen in the simulations with $\beta h/l = 1.39$ here. Only the one with the steepest slope exhibits separation.

The effect of the advection on the maximum concentration of the tracer is shown in figure 3(b) which plots the maximum surface concentration normalised on the value in the equivalent flat canopy simulation (c_{max}/c_{flat}) plotted against λ. Although the data does not collapse as well as figure 3(a) it is clear that for small values of λ where advection is small then (as expected) $c_{max}/c_{flat} \sim 1$ and concentrations vary little from those over a flat canopy. In contrast, for $\lambda > 5$ there is a larger spread in the values of c_{max}/c_{flat}. Maximum concentrations are increased - in this case by up to 50% in some simulations, although again the actual maximum value is not solely determined by λ. For a fixed canopy and hill width, then increasing the hill height (and hence the slope, H/L) leads to an increase in the maximum tracer concentration as a result of more pronounced differences in the eddy viscosity between the separation and reattachment points.

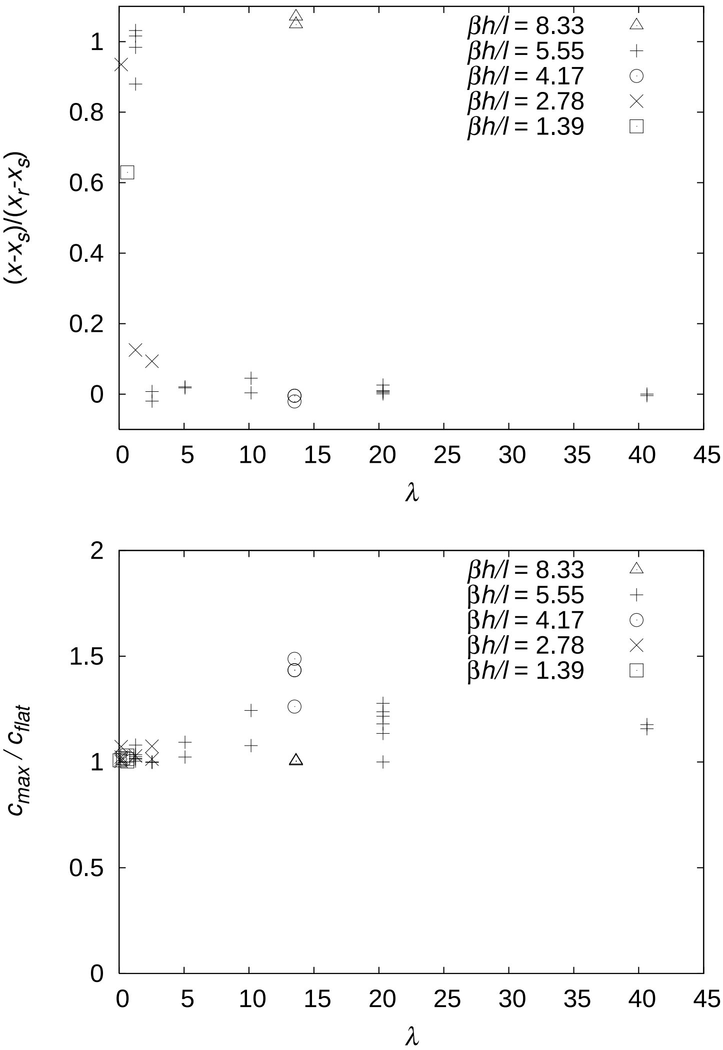

Fig. 3 (a) The non-dimension location of the scalar maximum relative to the separation region $\xi = (x_{trmax} - x_s)/(x_r - x_s)$ where x_{trmax} is the location of the maximum surface tracer concentration, x_s is the location of the separation point and x_r is the reattachment point plotted against vertical velocity parameter, λ for different non-dimensional canopy depths $\beta h/l$. (b) The maximum tracer concentration normalised on the value within the equivalent flat canopy plotted against λ.

A number of simulations were conducted with twice the horizontal and vertical resolutions to check the sensitivity of the results to model resolution. Doubling the resolution made no qualitative difference to the results. From a quantitative point of view there was almost no difference in the location of the separation region, or the maximum tracer concentrations deep in the canopy, although there was a slight increase in the calculated depth of the separation region with increased vertical resolution. Most sensitivity was observed at canopy top, where the strong vertical shear in the wind makes a high vertical resolution most necessary. Even here differences in canopy-top velocities and tracer concentrations were at most a few percent.

The conclusion of this analysis is that maximum concentrations almost always occur close to stagnation points. In the one-and-a-half order closer model the details of which separation point exhibits the highest concentration appears to be linked to the scale of the hill and the importance of vertical advection at canopy top. Smaller scale hills, where vertical advection is significant at canopy top, tend to exhibit minima of turbulent kinetic energy and eddy viscosity and maxima of tracer concentration at the separation point near the summit. Larger scale hills where canopy top vertical advection is smaller show the minima of turbulent kinetic energy and eddy viscosity and the maxima of tracer concentration at the reattachment point near the foot of the hill.

The details of which separation point exhibits the maximum tracer concentration are sensitive to small differences in the induced flow which lead to small differences in the turbulent kinetic energy and calculated eddy viscosity. The concentrations are therefore also likely to be sensitive to the details of the turbulence scheme. This is perhaps not surprising, but does mean that conclusions on the tracer concentrations in the deep canopy should be treated with some caution.

There are only a couple of simulations where the canopy is so shallow and sparse that no separation occurs at all. In these cases the maximum concentrations are observed near the foot of the hill similar to that observed in figure 2(b). At this location the adverse pressure gradient over the lee slope generates the lowest wind speeds and hence the eddy viscosity is smallest.

Above the canopy both the simulations in figure 2 exhibit horizontal variations in concentration. The scalar concentration isolines do not exactly coincide with the streamlines, suggesting that although advection plays an important role in modifying the scalar concentrations over the hill, turbulent fluxes are also important. The horizontal variations are larger over the small hill, as expected, since the vertical velocities are larger. These general features are also reproduced in the other simulations (not shown). The analysis of section 3 gives a scaling for canopy top perturbations in tracer concentration. Here the magnitude of the canopy top perturbations is characterised by the standard deviation of the canopy top scalar concentration. Figure 4 shows the standard deviation of the canopy top scalar concentration plotted against the scaling for the canopy top tracer perturbation, c. Results are plotted only for simulations with $H/L < 0.1$ and $L/L_c \geq 50$. This excludes the narrowest hills and steepest slopes where the Finnigan and Belcher (2004) model, and hence the tracer scaling, is not valid. Despite the fact that the analysis excludes the contribution to the variability from the deep canopy, the scaling does a good job in collapsing the data from a wide range of simulations with different canopies and hills. This suggests that canopy top

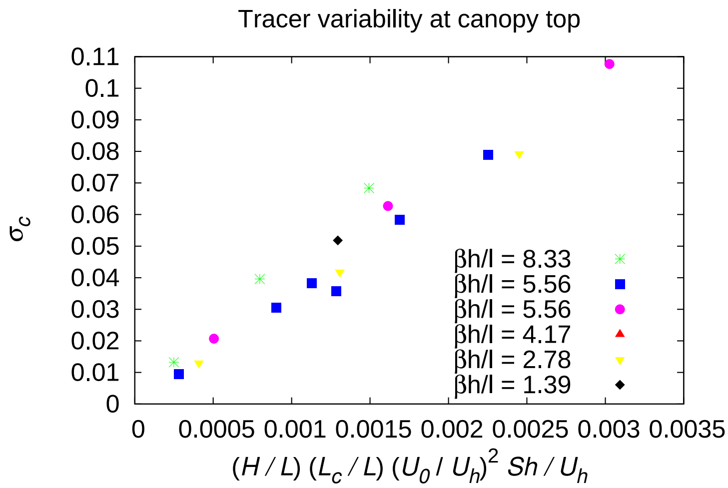

Fig. 4 The standard deviation of the tracer concentration at canopy top plotted against the scaling for tracer concentration from equation (12). Only experiments with $H/L < 0.1$ and $L/L_c \geq 50$ are included.

variations in tracer concentrations may not be overly sensitive to the deep canopy solution, and hence may well be successfully predicted by a mixing length turbulence closure scheme, unlike the deep canopy concentrations. For the narrower and steeper hills then vertical advection in the upper canopy plays an increasingly important role and the scaling appears no longer to hold (results not shown), with advection and the concentrations deeper in the canopy playing a bigger role.

Figure 5 shows the canopy top advection term for a number of different simulations. In Figure 5(a) the advection is non-dimensionalised on the source term and results are shown for a fixed canopy ($\beta h/l = 5.56$, $L_c = 10\,\mathrm{m}$) and slope ($H/L = 0.02$) and only the scale of the hill is changed. For the widest hills advection is small compared to the source term, while for the narrowest hill ($L = 100\,\mathrm{m}$) the advection term at canopy top is comparable in magnitude with the scalar source term in the canopy and so advection plays an important role, as might be expected. The other interesting feature is that advection is particularly important over the lee slope in the recirculation region which may be important for interpreting flux measurements over real forests. Figure 5(b) shows the advection over a range of different canopies and slopes for the widest hills ($L = 1600\,\mathrm{m}$). In this case advection is small compared to the source term and the scaling from (13) is expected to be valid. Results are shown non-dimensionalised on this scaling. The scaling is reasonably successful in collapsing the results over the range of canopies and slopes. For a fixed canopy but different slopes the collapse is excellent ($\beta h/l = 5.56$ and $L_c = 10\,\mathrm{m}$ with $H/L = 0.02$ or $H/L = 0.00625$). For different canopies the scaling broadly predicts the magnitude of the advection terms, but there are some in magnitude and in the phase which reflect the fact that the scaling ignores the contribution to the advection from flow deep in the canopy. Nonetheless the scaling is a useful means of predicting the importance of scalar advection in these wide hill cases where advection is relatively weak. The scaling is less successful in the narrow hill regime where advection becomes large (not shown).

These simulations using the one-and-a-half order turbulence closure scheme and a fixed source of tracer within the canopy all demonstrate that advection can be important in modifying tracer concentrations over canopy-covered hills. In particular, wherever there is significant vertical advection at canopy top (small hills / dense canopies / deep canopies) transport is enhanced. This transport leads to lower mean concentrations within the canopy and significant horizontal variations in tracer concentration. These variations can actually lead to localised increases in tracer concentration. The

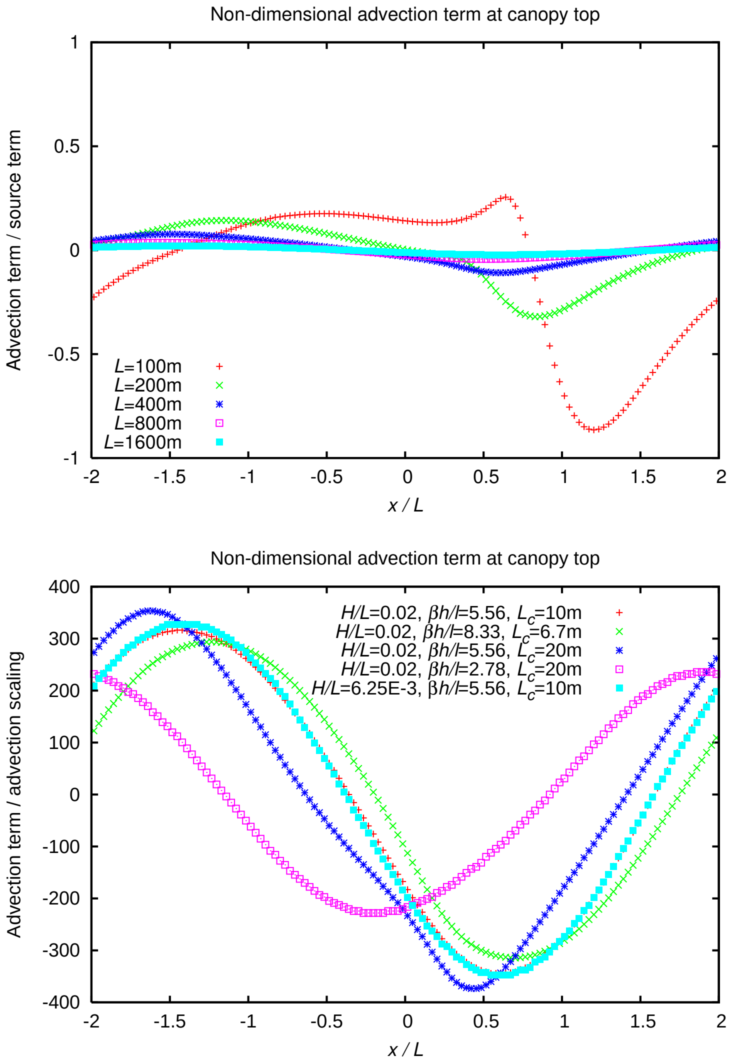

Fig. 5 Plots of the canopy top advection term as a function of non-dimensional distance across the hill for a number of different simulations. In (a) the slope and canopy are fixed ($H/L = 0.02$, $\beta h/l = 5.56$ and only the scale of the hill is changed ($L = 100 - 1600\,$m. In (a) the advection term is scaled on the source term, S. In (b) a number of different simulations with fixed width $L = 1600\,$m, but varying canopy and slope parameters are shown. The advection term is non-dimensionalised using the scaling in (13).

horizontal variations are closely linked to flow separation and recirculation within the canopy and therefore scaling parameters which quantify these dynamic effects are also useful in explaining different regimes of behaviour in tracer concentrations. A simple scaling argument based on the analytical solution for flow over a forested hill successfully collapses the observed tracer perturbations and also the tracer advection terms at canopy top over a wide range of simulations.

5 Large-eddy simulations

5.1 Large eddy simulations over a small hill

Simulations with the one-and-a-half order closure scheme are useful because the scheme is simple and therefore the simulations are quick to run. This allows a wide range of parameter space to be investigated. Given the uncertainties over mixing length closure schemes, and in particularly the sensitivity of tracer concentrations deep in the canopy to the turbulence scheme, then some form of validation of the results is however desirable. One way to address this is through the use of large eddy simulations. Such simulations are significantly more computationally expensive and therefore a limited number of simulations are possible, however they can help to validate conclusions drawn from the simpler one-and-a-half order closure scheme results.

Large eddy simulations of flow over both a flat surface and a small hill ($H = 10\,\mathrm{m}$, $L = 100\,\mathrm{m}$) are presented. The model setup is described in section 2.1 and is identical to that used in Ross (2008) with the addition of a passive tracer. Ross (2008) demonstrated that although some of the details of the flow, including the turbulence,

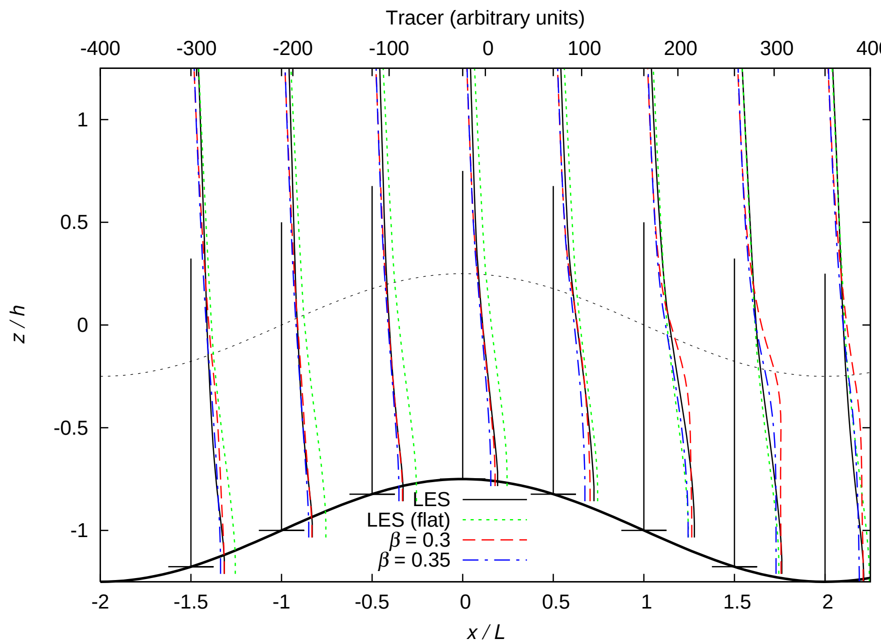

Fig. 6 Profiles of tracer (in arbitrary units) across a small hill from a LES simulation (solid black line), from a simulation using the one-and-a-half order closure scheme (red dashed line - $\beta = 0.3$ and blue dot-dashed line - $\beta = 0.35$). Also shown for comparison are the results from the LES over flat ground (green dotted line).

were different between LES and mixing-length simulations, the mean flow and broad dynamic features were in good agreement. This is primarily because the flow is dominated by turbulence generated in the shear layer at canopy top and this is well represented in the mixing-length scheme.

Figure 6 shows profiles of the scalar concentration across the hill. Results from the large-eddy simulations over the hill (solid black line) are compared with results from simulations using the one-and-a-half order closure scheme over the same hill and from the LES model over flat ground. The canopy, hill and flow parameters are the same in both the LES and one-and-a-half order closure simulations. The one-and-a-half order results are presented for two different values of the empirical parameter β. The value $\beta = 0.30$ corresponds to the value assumed in Finnigan and Belcher (2004) and Ross and Vosper (2005), while the value $\beta = 0.35$ was shown by Ross (2008) to better match the large-eddy simulation results in terms of the surface pressure field and wind speed and shear stress profiles. Here we see that all three simulations over the hill give very similar results in terms of scalar concentration profiles, suggesting that the scalar transport is not too sensitive to details of the turbulence scheme in this case. The results show small, but significant, differences from the results over flat ground. These differences are most noticeable over the upwind slope where mean-flow transport leads to lower concentrations deep in the canopy over the upwind slope compared to the flat case. Over the lee slope the concentrations in the recirculation region are slightly increased compared to the flat case, but the differences are smaller than over the upwind slope. Differences in the tracer profiles over the hill appear principally in the separation region over the lee slope. Again the value of $\beta = 0.35$ better reproduces the LES results, particularly near canopy top over the lee slope. Note that both values of β lie within the range of observed values from real forest canopies. These results are qualitatively similar to those observed using the one-and-a-half order closure scheme in section 2. A closer examination of the tracer concentrations shows that the region of high tracer concentration over the lee slope has a lower maximum and is more spread out in the LES simulation compared to the mixing length closure scheme. This is entirely consistent with figure 5(b) of Ross (2008) which showed that the LES predicted higher values for the turbulent kinetic energy in this region, and hence would be expected to exhibit more turbulent mixing. This probably reflects the fact that although there is little mean flow in the deep canopy there is significant variability in the flow and in the tracer concentrations resulting from the flow in the upper canopy and above penetrating down.

5.2 The turbulent Schmidt number

The first-order mixing length closure scheme assumes that the Reynolds shear stress, $\tau_{ij} = -\rho\overline{u_i'u_j'}$, and Reynolds-averaged turbulent tracer mixing term, $\overline{u_i'c'}$ are given by

$$\overline{u_i'u_j'} = K_m \left(\frac{\partial u_i}{\partial x_j} + \frac{\partial u_j}{\partial x_i}\right) \tag{15a}$$

$$\overline{u_i'c'} = K_c \frac{\partial c}{\partial x_i}. \tag{15b}$$

In the first order turbulence scheme K_m is determined using a mixing length closure. Ross (2008) examined the validity of this mixing length approximation for K_m using the LES results. Implicit in the first order mixing length closure is the assumption that the turbulent Schmidt number (the ratio of the turbulent diffusivities for momentum and scalar),

$$Sc \equiv \frac{K_m}{K_c} \tag{16}$$

is equal to 1, i.e. momentum and scalars are mixed by turbulence in exactly the same way. Experimental observations in the atmospheric boundary layer do not necessarily satisfy equation 15b for all components, i. In general K_m and K_c are defined to ensure that this is a reasonable approximation in the direction of the dominant turbulent flux. To calculate K_m and K_c from the LES data the vertical components are taken so

$$K_m = \frac{\overline{u'w'}}{\partial u/\partial z + \partial w/\partial x} \tag{17a}$$

$$K_c = \frac{\overline{w'c'}}{\partial c/\partial z}. \tag{17b}$$

In the boundary layer the Schmidt number is generally close to 1, however observations in forest canopies show that the Schmidt number decreases to about 0.5 in the reduced surface layer (RSL) which extends up to a few canopy heights above canopy top (Harman and Finnigan, 2008). This is also observed in the LES simulations over flat terrain (see figure 7). Within the canopy the LES then demonstrates a sharp increase in the Schmidt number up to a maximum of about 2 at a height of 5m above the ground, before it then decreases again towards the surface. Variations in the Schmidt number within the canopy are perhaps unsurprising as mixing-length closure schemes are known not to perform particularly well there (see e.g. Ross, 2008). From a dynamical point of view this has a relatively small impact since turbulent momentum fluxes are small deep within the canopy due to the small vertical wind shear. This is not necessarily the case for tracer fluxes, where there may still be significant gradients in tracer concentration.

Figure 7 also shows profiles of the Schmidt number derived from the large-eddy simulation at four different locations across the hill. These are slightly more noisy as averaging is only done in the lateral direction and over time on the hill, whereas streamwise averaging is also performed for the simulation over flat ground. All four profiles show similar trends to the results over flat ground with the Schmidt number decreasing from around 1 well above the canopy to a minimum near canopy top, and then increasing within the canopy to a maximum at about 5m above the ground. There are however significant quantitative differences between profiles.

Well above the forest canopy results are similar for all profiles. Closer examination of the turbulent diffusivities in figure 8 shows that both K_m and K_c are enhanced

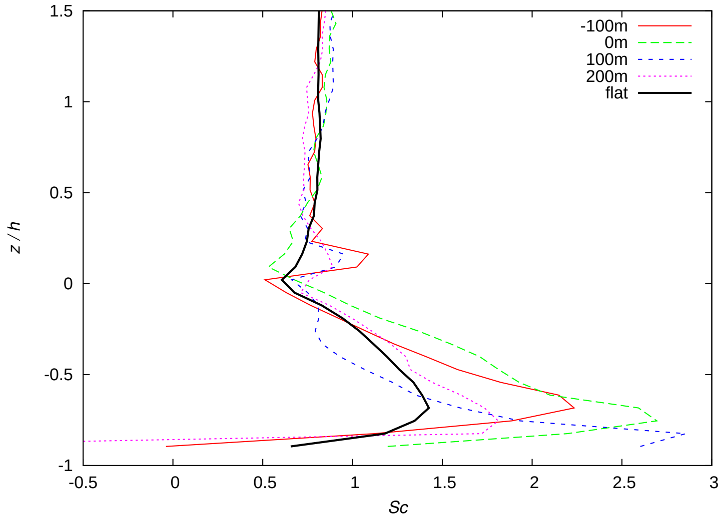

Fig. 7 Profiles of the turbulent Schmidt number on flat ground and at 4 locations over the hill derived from the large-eddy simulations. Canopy top is at $z/h = 0$.

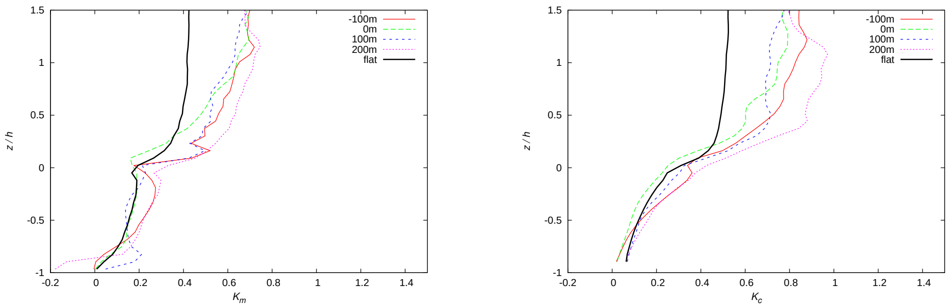

Fig. 8 Profiles of the turbulent diffusivity for (a) momentum, K_m and (b) tracer, K_c on flat ground and at 4 locations over the hill derived from the large-eddy simulations. Canopy top is at $z/h = 0$.

over the hill, but by similar amounts. This is due to increases in both the horizontally averaged momentum and scalar fluxes. This is perhaps slightly surprising and may be due in part to starting the LES averaging before the simulation has settled to a statistically stationary state. What is surprising is that despite these differences the calculated values of Sc above the canopy vary little over the hill and compare very well with the results over flat ground. The values of K_m and K_c increase particularly above the recirculation region ($x = 200\,\mathrm{m}$) in what is likely to be a real dynamic effect due to the hill. Just above canopy top the systematic variations between K_m and K_c compared to the flat case are smaller but there are much more significant differences in the Schmidt number with lower values than over flat ground at the summit of the hill and larger values elsewhere over the hill. The larger values of the Schmidt number in this region, up to values of about 1, are principally due to enhanced values of K_m in this region compared to over flat ground. This suggests that increased shear and vertical advection at canopy top are important in modifying turbulent transport just above the canopy, which is entirely in accord with the scaling analysis of section 3.

Within the canopy the Schmidt numbers over the hill exceed those over flat ground in most locations, and in particular the maximum values at low level are significantly larger, up to about 3. This is due to a combination of increased values of K_m over the lee slope (100m) and in the valley (200m) , and reduced values of K_c on the upwind slope (-100m) and near the summit (0m). The only place within the canopy where the Schmidt number is less over the hill than on flat ground is in the upper part of the canopy over the lee slope (100m). This is in the recirculation region, and the low wind shear in this region leads to reduced values of K_m compared to other parts of the canopy, although the impact on K_c is less.

What these large-eddy simulation results show is that the relationship between K_m and K_c is not simple within and above forest canopies. This particular small hill, where vertical advection is significant, is likely to be an extreme case, however this variability in the Schmidt number potentially makes modelling of tracer transport using mixing length closure schemes difficult. It would be possible to devise a scheme where *Sc* scaled with height to match results over flat ground, as done in Harman and Finnigan (2008), however these results suggest that even this approach might not be sufficient over hills. Having said all this it is then perhaps surprising that the tracer profiles from the one-and-a-half order model agree so well with those from the LES in figure 1. Perhaps this suggests that tracer advection is actually dominating in these cases and so errors in turbulent tracer fluxes are less important. This does seem to agree with the conclusions of the scaling analysis in section 3 that the leading order perturbation in the turbulent fluxes is zero. This is clearly a topic for further research in terms of modelling scalar transport within and above forest canopies over complex terrain. In particular it would be interesting to run large eddy simulations for much wider hills where advection is smaller and hence turbulent transport is more important, however computational requirements preclude this with the current version of the model described here.

6 Implications for flux measurements

Observations of carbon uptake by forests are frequently made using eddy-covariance flux measurements on a large tower (e.g. the FLUXNET project Baldocchi et al., 2001) and assuming that this is representative of a forest. Many forested sites are not truly flat though and so the assumptions of horizontal homogeneity are not exactly met. The potential impact of advection on the flux measurements has to be considered. Night-time drainage flows on even gentle slopes are an often-cited source of errors in flux measurements (e.g. Wilson et al., 2002; Belcher et al., 2008), however this work shows that even under neutral, strong wind conditions advection may be non-negligible. There is evidence of this from the FLUXNET sites. The study of Wilson et al. (2002) demonstrated an average imbalance of around 20% in the energy balance, even in daytime conditions. The imbalance was observed even for well-mixed conditions (i.e. more neutral flow with stronger winds), although it increased for lower wind speeds and was much larger in nocturnal conditions. The advective effects demonstrated by this work, even for large hills with relatively small slopes, are certainly consistent with these observations. Figure 9 shows the turbulent scalar flux (non-dimensionalised on the depth integrated scalar source term) at canopy top and height h above the canopy for three different hills with the same slope ($H/L = 0.1$), but different scales ($L = 100, 200, 400, 1600$). In each case the canopy and the uniform scalar source term are the same ($\beta h/l = 5.55$, $L_c = 10\,\mathrm{m}$, $S = 10^{-2}\,\mathrm{m}^{-3}\,\mathrm{s}^{-1}$). For steady-state flow over flat ground the non-dimensional scalar flux is one since production in the canopy is balanced by turbulent transport at canopy top. For the widest hill, with relatively weak canopy-top vertical velocities the canopy-top scalar fluxes only vary a small amount across the hill. Note that the total flux integrated across the hill is slightly less than the flat ground case, suggesting that advection is responsible for a small net transport of scalar out of the canopy. As the scale of the hill decreases the variability in the canopy-top fluxes increases significantly. At some points over the smallest hill point measurements of the canopy top turbulent flux vary by up to a factor of three compared to the source term. Variations at a height h above the canopy are qualitatively similar, but smaller in magnitude than those at canopy

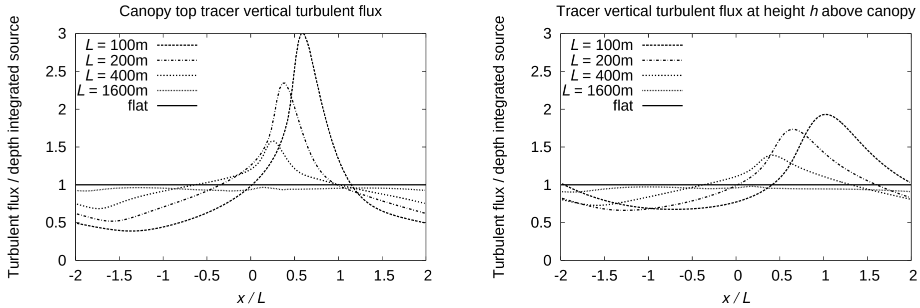

Fig. 9 Canopy-top turbulent scalar flux (normalised on the depth-integrated canopy source term) plotted against the position across the hill (non-dimensionalised on the hill width) for different hills (simulations 3, 5 and 7 in §2).

top. The increased height above the canopy smooths out some of the canopy-induced variability. For the smallest hill there is still a difference of up to a factor of two compared to the flat-ground case.

A further consideration when interpreting flux measurements is that the flow into and out of the canopy means that streamlines are not parallel to the terrain or to canopy top, and therefore techniques which rotate sonic anemometer measurements into a mean flow coordinate system or use a planar fit to the flow data as a coordinate system (see e.g. Lee et al., 2004) may not give the expected results. In particular, the lack of symmetry to a reversal of wind direction means that even for an ideal symmetrical hill and ideal conditions the averaged wind data will not lie in a plane. For large-scale hills the effect will be relatively small, but for smaller scale hills it could be significant.

Modelling studies such as these are not yet practical for correcting or scaling observational flux measurements for the effects of terrain, however they do provide important indications of the type and magnitude of errors that may be introduced through neglecting such effects. They may also provide guidance into the most suitable locations for making flux measurements which are truly representative of a larger area.

7 Conclusion

This paper provides a systematic investigation of the impact of hills on scalar concentration and transport within and above a forest canopy. With a fixed uniform source of scalar within the canopy the dynamics of the canopy - boundary layer interactions (previously studied by e.g Finnigan and Belcher, 2004; Ross and Vosper, 2005) dominate. Over hills the pressure field resulting from the presence of the hill drives flow into and out of the canopy and this dynamical process acts like a pump to remove scalars more efficiently from the canopy space. This reduces the mean concentration of scalar within the canopy for a fixed source term. This effect is particularly strong for small-scale hills where the canopy-atmosphere mean flow is largest. Although the overall effect is to reduce mean scalar concentrations in the canopy, there is a large spatial variability in concentrations in the canopy, with the maximum concentrations at a given canopy depth often exceeding those over flat ground. This is closely linked to flow separation in the lee of the hill trapping scalars in the canopy. In cases where there is moderately strong vertical advection at canopy top then the maximum concentrations occur near the separation point. Low wind speeds and shear in this region result in weak turbulent transport and long canopy residence times for the air, which both contribute to higher scalar concentrations. While these broad features are relatively robust it is likely that the details of tracer concentrations in the canopy will be sensitive to the turbulence closure scheme. Canopy top tracer variations can be successfully predicted using a simple scaling argument which neglects the deep canopy. This works well for relatively wide hills and suggests that in these cases first order closure schemes may be more successful than anticipated in predicting tracer concentrations. Similar results for time-averaged scalar concentrations are seen for a large-eddy simulation of flow over a small hill based on the simulations in Ross (2008). The LES does highlight the unsteady and intermittent nature of the flow in the canopy. Calculations of the Schmidt number in the LES also suggest that the common assumption that momentum and scalars are transported in the same way is not valid within and just above the canopies, with significant variations in the Schmidt number in the vertical and across the hill. In principle at least some of this variability could be represented with a parametrisation of the Schmidt number in the canopy, but whether this is the most significant source of uncertainty in mixing length closure models for canopy flows remains to be studied.

Acknowledgements This work was partially supported by the UK Natural Environment Research Council (NERC) through grant NE/C003691/1. The author would like to thank the anonymous reviewers who's thorough comments significantly improved this paper.

References

Baldocchi D, Falge E, Gu LH, Olson R, Hollinger D, Running S, Anthoni P, Bernhofer C, Davis K, Evans R, Fuentes J, Goldstein A, Katul G, Law B, Lee XH, Malhi Y, Meyers T, Munger W, Oechel W, Paw U KT, Pilegaard K, Schmid H, Valentini R, Verma S, Vesala T, Wilson K, Wofsy S (2001) FLUXNET: A new tool to study the temporal and spatial variability of ecosystem-scale carbon dioxide, water vapor, and energy flux densities. Bull Amer Met Soc 82:2415–2434

Belcher SE, Finnigan JJ, Harman IN (2008) Flows through forest canopies in complex terrain. Ecol Apps 18:1436–1453

Brown AR, Hobson JM, Wood N (2001) Large-eddy simulation of neutral turbulent flow over rough sinusoidal ridges. Boundary-Layer Meteorol 98:411–441

Dupont S, Brunet Y, Finnigan JJ (2008) Large-eddy simulation of turbulent flow over a forested hill: Validation and coherent structure identification. Quart J Roy Meteorol Soc 134:1911–1929

Feigenwinter C, Bernhofer C, Eichelmann U, Heinesch B, Hertel M, Janous D, Kolle O, Lagergren F, Lindroth A, Minerbi S, Moderow U, Mölder M, Montagnani L, Queck R, Rebmann C, Vestin P, Yernaux M, Zeri M, Ziegler W, Aubinet M (2008) Comparison of horizontal and vertical advective CO2 fluxes at three forest sites. Agric For Meteorol 148(1):12–24

Finnigan JJ (2000) Turbulence in plant canopies. Annu Rev Fluid Mech 32:519–571

Finnigan JJ (2008) An introduction to flux measurements in difficult conditions. Ecol Apps 18(6):1340–1350

Finnigan JJ, Belcher SE (2004) Flow over a hill covered with a plant canopy. Quart J Roy Meteorol Soc 130:1–29

Finnigan JJ, Brunet Y (1995) Turbulent airflow in forests on flat and hilly terrain. In: Coutts MP, Grace J (eds) Wind and trees, Cambridge University Press, pp 3–40

Harman IN, Finnigan JJ (2008) Scalar concentration profiles in the canopy and roughness sublayer. Boundary-Layer Meteorol 129(3):323–351

Hunt JCR, Leibovich S, Richards KJ (1988) Turbulent shear flow over low hills. Quart J Roy Meteorol Soc 114:1435–1470

Katul GG, Mahrt L, Poggi D, Sanz C (2004) One- and two-equation models for canopy turbulence. Boundary-Layer Meteorol 113:81–109

Katul GG, Finnigan JJ, Poggi D, Leuning R, Belcher SE (2006) The influence of hilly terrain on canopy-atmosphere carbon dioxide exchange. Boundary-Layer Meteorol 118:189–216

Lee X, Massman W, Law B (eds) (2004) A handbook of micrometeorology: A guide for surface flux measurements. Kluwer academic publishers

Patton EG, Katul GG (2009) Turbulent pressure and velocity perturbations induced by gentle hills covered with sparse and dense canopies. Boundary-Layer Meteorol 133:189–217

Pinard JDJP, Wilson JD (2001) First- and second-order closure models for wind in a plant canopy. J Appl Meteor 40(10):1762–1768

Poggi D, Katul GG (2007a) The ejection-sweep cycle over bare and forested gentle hills: a laboratory experiment. Boundary-Layer Meteorol 122:493–515

Poggi D, Katul GG (2007b) An experimental investigation of the mean momentum budget inside dense canopies on narrow gentle hilly terrain. Agric For Meteorol 144:1–13

Poggi D, Katul GG (2007c) Turbulent flows on forested hilly terrain: the recirculation region. Quart J Roy Meteorol Soc 133:1027–1039

Ross AN (2008) Large eddy simulations of flow over forested ridges. Boundary-Layer Meteorol 128:59–76

Ross AN, Vosper SB (2005) Neutral turbulent flow over forested hills. Quart J Roy Meteorol Soc 131:1841–1862

Wilson K, Goldstein A, Falge E, Aubinet M, Baldocchi D, Berigier P, Bernhofer C, Ceulmans R, Dolman H, Field C, Grelle A, Ibrom A, Law BE, Kowalski A, Meyers T, Moncrieff J, Monson R, Oechel W, Tenhunen J, Valentini R, Verma S (2002) Energy balance closure at FLUXNET sites. Agric For Meteorol 113:223–243

Wood N, Mason PJ (1993) The pressure force induced by neutral, turbulent flow over hills. Quart J Roy Meteorol Soc 119:1233–1267

Zeri M, Rebmann C, Feigenwinter C, Sedlak P (2010) Analysis of short periods with strong and coherent CO2 advection over a forested hill. Agric For Meteorol 150(5):674–683